Study of fouling in two-stage reverse osmosis desalination unit operating without an inlet pH adjustment: diagnosis and implications

Khaled Touati, Mehdi Hila, Kalthoum Makhlouf and Hamza Elfil

ABSTRACT

In the current work, the diagnosis of a reverse osmosis desalination unit is reported. Over the two last decades, the studied desalination unit was supplying a 1,200 bed hotel. The feed water was driven from a well near the sea. The desalination unit has two stages giving an average recovery equal to 81%. The behaviour of all water streams with respect to aggressiveness and scaling tendency was assessed. The second stage reject water was shown to exhibit a very high scaling behaviour with an instantaneous precipitation in the absence of feed water pH adjustment. The analyses have shown that the produced water was very aggressive. The second stage module autopsy has revealed a sharp decrease in the membrane performances because of mineral as well as organic fouling. The inorganic scale was essentially made of coesite, calcite and kaolinite clay. The presence of silica and clay was attributed to an inadequate pre-treatment process, whereas the presence of calcite crystals at the membrane surface reveals that the chemical inhibition performed at the pre-treatment process without adjusting the pH was not able to prevent calcium carbonate precipitation. A periodic acid wash of the second stage membranes is then necessary to guarantee the desired objectives of this stage.

Key words | calcium carbonate, desalination, fouling, membrane autopsy, reverse osmosis

Khaled Touati (corresponding author)
Hamza Elfil
Laboratory of Natural Water Treatment,
Center of Researches and Water Technologies,
B.P. 273,
Soliman 8020,
Tunisia
E-mail: *kha.touati@gmail.com*

Mehdi Hila
PROMOLAB, Appart A,
193 Av. Hbib Bourguiba,
2033 Megrine,
Tunisia

Kalthoum Makhlouf
Laboratory of Thermal Processes,
Center of Researches and Energy Technologies,
B.P. 95,
Soliman 2050,
Tunisia

INTRODUCTION

In the last few years, the use of small reverse osmosis (RO) water desalination units has sharply increased. Their use covers several economic sectors: industry, agriculture, and hostelry. In Tunisia, more than 100 small capacity reverse osmosis water desalination (ROWD) units (500 to 2,000 m^3/d) have already been installed in hostels throughout the country. However, many of these units have seen a drastic decrease in their performances. Indeed, their use is hindered by several phenomena such as concentration polarization and fouling, which lead to an increased operating cost and a decreased quality and quantity of the produced water (Ning *et al.* 2005). In some cases repeated problems with sections of the treatment process have led to the shutdown of parts of key units or even the whole units. Fouling is the major contributor to RO units operating problems. Fouling is defined as the build-up of a layer on the surface of the RO membrane. The deposited layer could be of colloidal, mineral or organic or bioorganic origin. The added layer will decrease the membrane permeability and therefore the unit yields (Ivnitskya *et al.* 2005). Fouling consequences include reduction in the membrane lifespan; decrease in the permeate flux; decrease in the membrane salt rejection rate; increase in the pressure drop; and decrease in the driving force. The operating conditions of the installed ROWD units do not help to avoid fouling or even identify the cause of fouling. Indeed, these units are generally operated by non-qualified people. Moreover, they are not usually equipped with the necessary measuring devices (pH sensor, conductivity sensor, pressure sensor, etc.). In such situations, default revealing and scaling

doi: 10.2166/ws.2017.067

prevention or even scaling detection since its earliest appearance will be extremely difficult. Any antiscalant injection mishandling may lead to $CaCO_3$ nucleus formation which will provoke calcium carbonate scaling even in the presence of chemical inhibitors (Elfil *et al.* 1998), especially when the membrane is not periodically and effectively acid washed. With the lack of adequate control equipment that will maintain the optimal operating trend and detect any defect, the unit diagnosis is the only available means of discovering the causes of the performances decrease (Boubakri & Bouguecha 2008). The diagnosis is based on the analysis of all water fluxes (feed, reject, permeate) and membrane autopsy. Water analysis is mainly conducted to assess the fouling and scaling behaviour. Autopsy is performed to identify the deposited matter on the membrane surface (Tran *et al.* 2007; Ben Hamouda *et al.* 2014). In the current work, the diagnosis of a ROWD unit is performed. The unit was installed in 1997 to produce 45 m^3/h of desalinated water for a 1,200 bed hotel. The two-stage unit is fed from a coastal well providing a water quality with 6 $g{\cdot}L^{-1}$ total dissolved solids (TDS). In this case, the inlet water pH was not adjusted. The second unit stage revealed a drastic decrease in its performances. To overcome the conversion rate decline, the pressure head was increased in the second stage which increased the water desalination cost. It is worth noting that, due to mismanagement, sensors and equipment failings, the unit operation history is totally unknown and the operating data are non-existent. The diagnosis will be then based on water characteristics and deteriorated module autopsy.

THEORETICAL BACKGROUND

In the desalination field, two scaling indices are usually used to assess the scaling tendency of brine water. While the Langelier Saturation Index (LSI) (Langelier 1936) is often applied for brine solutions of a TDS not exceeding 10 g/L, the Stiff and Davis Saturation Index (SDSI) (Stiff & Davis 1952) is used to assess the scaling tendency of highly saline solutions such as those encountered in sea water desalination. To evaluate the scaling behaviour of any kind of water, scaling indices are usually used. Most stability indices used in the literature are based on the determination of saturation pH (pHs). The expression of the pHs is formulated by combining the equation of the solubility product, K_s, with the equilibrium relation of the second ionization of the carbonic acid, K_2:

$$K_s = (Ca^{2+})(CO_3^-) \tag{1}$$

$$K_2 = \frac{(CO_3^{2-})(H_3O^+)}{(CO_3^{2-})} \tag{2}$$

Combining Equations (1) and (2) with application of logarithm yields:

$$\mathrm{pH_S} = \mathrm{pK_2} - \mathrm{pK_S} - \log\gamma_{Ca^{2+}} - \log\gamma_{HCO_3^-} - \log[\mathrm{Ca^{2+}}] - \log[\mathrm{Alc}] \tag{3}$$

where $[Alc]$ is the concentration of the alkalinity which is assimilated to the concentration of HCO_3^- at solution pH < 9 ($[\mathrm{Alc}] \approx [HCO_3^-]$). The LSI is then defined as follows:

$$LSI = \mathrm{pH_{mes}} - \mathrm{pH_s} \tag{4}$$

where $\mathrm{pH_{mes}}$ is the measured pH of the treated solution, and $\mathrm{pH_s}$ is the pH of saturation with respect to calcite, defined as:

$$\mathrm{pH_S} = \mathrm{pK'_2} - \mathrm{pK'_S} - \log[\mathrm{Ca^{2+}}] - \log[\mathrm{Alc}] - log[1 + 2.10^{pK'_S - pK'_2}] \tag{5}$$

$\mathrm{pK'_2}$ and $\mathrm{pK'_S}$ are defined as the apparent constants of the second dissociation of carbonic acid and the solubility product of calcite at a given ionic strength. It is clearly seen that LSI uses the concentrations instead of activities. At pH < 9.5, the term $1 + 2.10^{pK'_S - pK'_2}$ is neglected. Then, the LSI expression becomes:

$$\mathrm{pH_S} = \mathrm{pK'_2} - \mathrm{pK'_S} - \log[\mathrm{Ca^{2+}}] - \log[\mathrm{Alc}] \tag{6}$$

Similar to the LSI formula, the SDSI is presented as follows:

$$\mathrm{SDSI} = \mathrm{pH_{mes}} - \mathrm{pH_s} \tag{7}$$

$$\mathrm{pH_s} = -\log[\mathrm{Ca^{2+}}] - \log[\mathrm{Alc}] + K \tag{8}$$

where K is an empirically determined constant which is associated with the ionic strength. Experimental investigations have shown that the calcite which is considered to be the most stable form of the six calcium carbonate allotropic varieties is not involved in the $CaCO_3$ nucleation (Gal *et al.* 2002). Actually the $CaCO_3$ hydrated forms [(amorphous calcium carbonate (ACC); monohydrate calcium carbonate (MCC) and not the anhydrous forms (calcite, aragonite and vaterite)] were revealed to be crucial precursors for calcium carbonate spontaneous nucleation. The solubility products of the MCC and the ACC were proven to constitute lower limits for spontaneous and instantaneous nucleation respectively in the temperature interval ranging between 20 and 60 °C (Elfil & Roques 2001). According to these facts, between 25 and 60 °C, the MCC solubility product constitutes a lower limit that must be exceeded to obtain a spontaneous germination (Elfil & Roques 2004). The saturation pH is calculated using the $CaCO_3.H_2O$ solubility product instead of that relative to calcite. For a pH ranging between 6 and 9, it is written as:

$$pH_{s/MMC} = pK_2 - pK_{s/MMC} - \log\gamma_{Ca^{2+}} - \log\gamma_{HCO_3^-} - \log[Ca^{2+}] - \log[Alc] \quad (9)$$

where $pH_{S/MCC}$ and $pK_{S/MCC}$ are respectively the MCC saturation pH and solubility product. Similar to the previous indices, the MLSI is then defined as follows (Elfil & Hannachi 2006):

$$MLSI = pH - pH_{S/MCC} \quad (10)$$

The activity coefficients are calculated by simple models, such as 'Modified Debye & Hückel' for solutions with an ionic strength of less than 0.2 M (or TDS <10 g/L). For more saline waters, such as seawater desalination by RO, more complex models are valid as Simplified Pitzer (FI <2 M). $MLSI_{inst} < MLSI$; Water is highly scaling and the phenomenon is instantaneous (at 30 °C: $MLSI_{inst} = 0.74$).

- $0 < MLSI < MLSI_{inst}$; Water is scaling; the phenomenon depends on the wall nature and will be slow for MLSI values close to 0.
- $MLSI_{agr} < MLSI < 0$; There is no spontaneous precipitation; water is at a Ca-carbonic equilibrium (at 25 °C: $MLSI_{agr} = -1.33$).
- $MLSI < MLSI_{agr}$; Water is under saturated with respect to calcite and can be considered as aggressive.

The $MLSI_{inst}$ is given by the same Equation (9) when substituting $pH_{S/MCC}$ by the ACC saturation pH, $pH_{S/ACC}$. Surpassing this value is an indication of a highly scaling behaviour as the ACC was shown to be a precursor for $CaCO_3$ nucleation at high supersaturation (Elfil & Roques 2004). $MLSI_{agr}$ is also given by Equation (9) when replacing the $pH_{S/MCC}$ by the calcite saturation pH, $pH_{S/calcite}$, which is exactly the saturation pH defined by Langelier (Langelier 1936).

MATERIALS AND METHODS

Analytical techniques

X-ray diffraction

X-ray diffraction (XRD) was used to identify the precipitate formed. The diffractometer used was 'Philips X'Pert PRO' brand that has a vertical goniometer (θ-2θ) configuration with direct optical coding for direct reading of the angular position of the goniometer arm and having a remarkable absolute angular precision of 0.0025° and a repeatability of less than 0.0001°. It is equipped with an X-ray tube with a copper anti-cathode providing a bi-chromatic radiation wavelengths Cu-$\lambda K_{\alpha 1} = 1{,}540{,}598$ Å and Cu-$\lambda K_{\alpha 2} = 1{,}544{,}426$ Å and ceramic technology, a door sample rotating combined with auto-sampler and a X'Celerator detector associated with a secondary mono-chromator.

Scanning electron microscope

The scanning electron microscope used in the current study is the QUANTA 200Tare model (FEI Company). It was utilized to characterize the morphology of the deposit.

Infrared spectroscopy

Approximately 5 mg of each sample is ground with 400 mg dried KBr. The mixture was used to collect infrared (IR)

spectra. The IR spectra were collected using Fourier transform infrared (FTIR) spectrometer IRAffinity-1 (Shimadzu, Japan). The spectral region was 4,000–400 cm^{-1} and the spectral resolution used was 2 cm^{-1}. Every sample was prepared and consequently measured three times. The mean IR spectra were obtained using subsequent statistical processing.

Description of the two-stage RO unit

The RO desalination unit was commissioned in 1997 to satisfy a hotel requirement for treated water mounting to 45 m^3/h approximately. The treated water is used for several purposes: irrigation, showers, laundries, swimming pools, fire cycle water. The desalinated water was not used as a drinking water. The RO water desalination unit (Figure 1) was fed from a coastal well, about 300 m distant from the sea, providing brackish water with 6.2 $g{\cdot}L^{-1}$ salinity. In this unit, water undergoes a pretreatment before passing through the RO modules arranged in two stages. Before exiting the unit, a post treatment is performed. The unit was also equipped with a circuit for washing the RO membranes.

The pretreatment is carried out in two steps, as follows. (1) Sand filtration to retain suspended matter and colloids; antiscalant post injection to avoid calcium carbonate and gypsum scaling within the membranes. (2) A 5 μm cartridge filter trap fine particles (>0.1 μm). In the first stage, 30 RO modules are arranged in five sets. These modules are Trisep ACM8040 Spiral wound type polyamide modules. The second stage has also the same RO modules number. However the later modules are Filmtec SW30 type. The 57 m^3/h inlet water flow rate is pumped at a pressure of 21 bars. The first stage has a recovery rate of 67% and provides 82% of the desalinated water need with 300 mg/L salinity. The reject flux, having a salinity of 18 $g{\cdot}L^{-1}$, is pumped to the second stage at a 32 bars pressure. This stage provides 8 m^3/h permeate flux with a 400 $mg{\cdot}L^{-1}$ TDS and a 42% conversion rate. The total desalinated water flow rate is 45 m^3/h. The overall conversion rate is

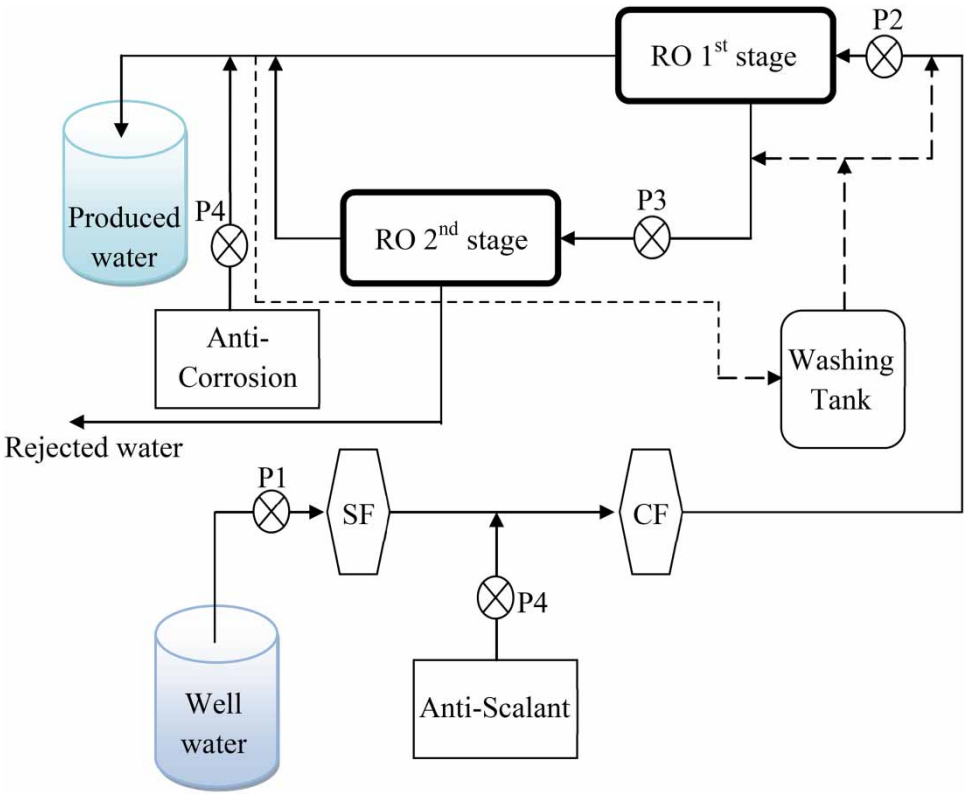

Figure 1 | Schematic description of the two-stage desalination unit. (P1: Feed pump; P2: first stage high pressure pump; P3: second stage booster pump; P4: dosing pump; SF: sand filter; CF: cartridge filters).

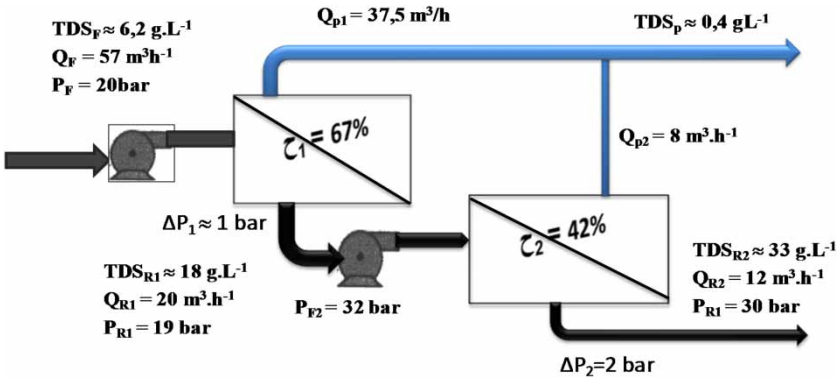

Figure 2 | RO modules feed and outlet data.

approximately 81% and the permeate salinity is well below 400 mg·L^{-1} (Figure 2). The reject flux, 12 m^3/h of water with 33 g·L^{-1} TDS, is thrown into the sea. The permeate goes through a post-treatment operation where the pH is adjusted and a corrosion inhibitor is added. The RO membranes are periodically chemically cleaned and washed.

EXPERIMENTAL RESULTS

Scaling/equilibrium/aggressive: behaviour of water fluxes

As presented in Table 1, the physico-chemical properties of each water stream are illustrated. Therefore, the scaling or aggressive behaviour of all the water qualities within the desalination unit can be assessed. Calcium carbonate saturation indices, and calcium sulfate and SiO_2 super-saturations for all water fluxes have been calculated and shown in Table 2. The scaling behaviours, with respect to the $CaCO_3$, are presented in the calco-carbonic diagram (Figure 3).

Feed water

According to the MLSI values, as clearly shown in Figure 3, the inlet water is at calco-carbonic equilibrium, even when it is in contact with atmospheric air (until pH = 7.9). The LSI and SDSI indices (Table 2) predict scaling water behaviour with respect to $CaCO_3$. However, no evidence of this is shown in the pretreatment section. The feed water is

Table 1 | Properties of the desalination unit water fluxes

	Feed	1st stage reject	2nd stage reject	1st stage permeate	2nd stage permeate
pH	6.8	7.5	7.6	6.12	6.36
T (°C)	22	22.9	23.7	23	23.7
Cond (μS·cm^{-1})	9,840	19,400	45,700	398	581
TDS (mg/L)	6,160	17,487	32,232	268	388
Ca^{2+} (mg/L)	412	1,300	2,280.0	3.7	12.0
Mg^{2+} (mg/L)	165.3	448.9	950.3	3.4	4.2
Na^{+} (mg/L)	1,600	4,606	8,840.9	86.8	101.1
K^{+} (mg/L)	24.8	64.4	110.4	1.2	1.2
Cl^{-} (mg/L)	2,650	8,012	15,666.0	132.5	160.0
SO_4^{2-} (mg/L)	996	2,988	4,696.0	10.0	14.9
HCO_3^{-} (mg/L)	368.4	1,122.4	1,976.4	15.7	23.3
Fe^{2+} (mg/L)	0.02	–	–	–	–
Al^{3+} (mg/L)	0.09	–	–	–	–
Mn^{2+} (mg/L)	0.1	–	–	–	–
SiO_2 (mg/L)	16	–	–	–	–

Table 2 | $CaCO_3$ saturation indices and $CaSO_4$ and SiO_2 supersaturation values of the RO desalination unit water streams

	Feed	1st stage reject	2nd stage reject	1st stage permeate	2nd stage permeate
MLSI	−1.0	0.4	1.0	−4.7	−4.0
SDSI	0.1	1.2	1.7	–	–
LSI	0.4	2.1	2.6	−3.8	−2.9
$\Omega_{/Gypsum}$	0.3	1.4	2.3	–	–
$\Omega_{/SiO2}$	0.13	0.41	0.73	–	–
Ionic strength	0.131	0.387	0.867	0.004	0.006

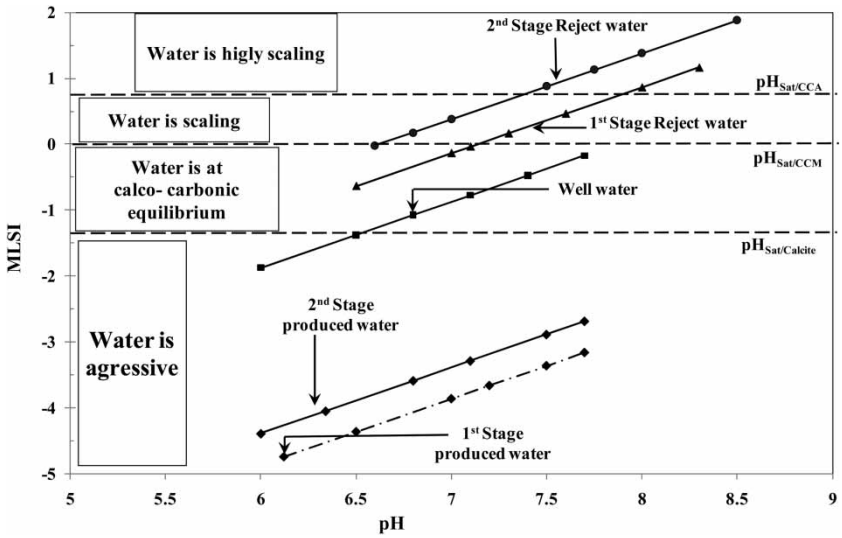

Figure 3 | Calco-carbonic diagram: Assessment of the $CaCO_3$ scaling/aggressive behaviour of the unit water flux for various pH values at 25 °C.

under saturated with respect to gypsum ($\Omega_{/Gypsum} = 0.3$) and to silicate ($\Omega_{/SiO2} = 0.13$).

First stage reject water (second stage feed water)

The first stage reject water has a TDS of nearly 18 $g{\cdot}L^{-1}$ and a pH value of 7.5. At this pH, water exhibits a slightly scaling behaviour as predicted by the MLSI (Figure 3). Indeed, the measured pH values are between saturation pH values of $CaCO_3{\cdot}H_2O$ ($pH_{Sat/CCM}$) and those of $CaCO_3$ amorphous form ($pH_{Sat/CCA}$). Under these conditions, antiscalant injection of VITTEC 3000 is sufficient to prevent calcium carbonate scale buildup in the first stage without the need to add acid for pH adjustment. However, the LSI and SDSI values, 2 and 1 respectively (Table 2), predict a much higher scaling behaviour probably advocating the need for a pH adjustment in the pretreatment phase. The first stage reject water presents a low supersaturation with respect to gypsum ($\Omega_{/Gypsum} = 1.4$) and the presence of an antiscalant would cut any gypsum scaling risk. The first stage reject water is below saturation with respect to silica ($\Omega_{/SiO2} = 0.41$).

Second stage reject water

The second stage reject flux has a salinity of 33 $g{\cdot}L^{-1}$ and a pH of 7.6. The calcium and alkaline hardness are approximately 2.3 and 2.0 $g{\cdot}L^{-1}$ respectively. These very high values predict a highly scaling water behaviour and $CaCO_3$ precipitation is instantaneous above a pH of 7.4 as suggested by calco-carbonic diagram (Figure 3) and saturated indices values (Table 2). Despite the use of a chemical inhibitor, calcium carbonate scaling was not prevented as the deposit on the surface of the membrane contained Calcite. In such case, scaling will only be prevented when combining chemical inhibition and water acidification.

Super-saturation with respect to gypsum is approximately equal to 2.3. This value is well below the limiting value ($\Omega_{/Gypsum} = 3$) above which the VITTEC 3000 is no longer efficient in preventing Gypsum scaling. The second stage reject water is below saturation with respect to silicate ($\Omega_{/SiO2} = 0.73$).

Produced waters

The first and second stage permeates have a very low TDS (<0.4 $g{\cdot}L^{-1}$) with pH values of respectively 6.1 and 6.4. The calcium and alkaline hardness are considerably low (see Table 1). The corresponding LSI values for the first and the second stages are −3.8 and −2.9, respectively. These negative values are a clear indication that the permeates are very aggressive. This is also shown on the calco-carbonic diagram (Figure 3). This aggressiveness prompts

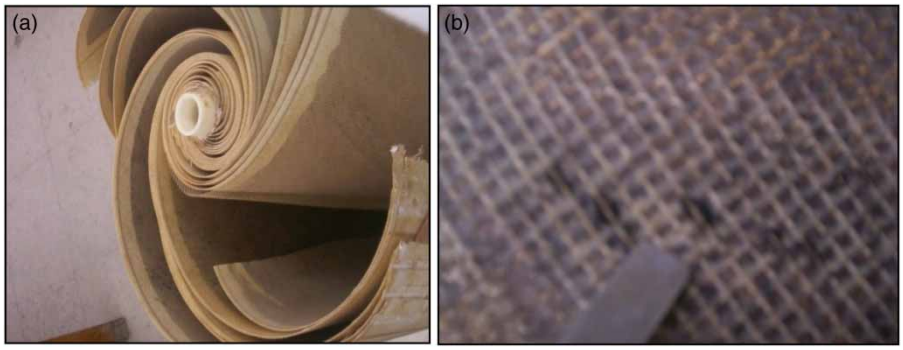

Figure 4 | Appearance of second stage membrane surface.

corrosion in the permeate water circuit. Consequently, a chemical intervention to avoid corrosion is needed, that is why a post-treatment for pH adjustment was planned. A corrosion inhibitor is then added (VICAOUT 3000). This complementary treatment will only contribute to limiting the corrosion phenomenon.

The LSI and the SDSI, which are often used to assess the scaling tendency in the desalination field, are not able to predict the calco-carbonic equilibrium state under specific conditions (Elfil & Hannachi 2006). Experimental evidence showed in many published works (Elfil & Hannachi 2006; Hannachi 2007) that the $CaCO_3$ scaling involves necessarily a precursor. The MLSI, which embeds the referred thermodynamic aspects of the CO_2-H_2O-$CaCO_3$ system, was consistent with the experimental evidence in the case of saline as well as highly saline waters. This index can substitute the traditionally used saturation indices (LSI, SDSI, etc.) for scaling tendency assessment for various water fluxes in the RO desalination processes.

Second stage membrane autopsy

The most convenient method to determine the organic, mineral, and microbiological condition of the membranes is to carry out destructive autopsy procedures to analyze foulants in the membrane surface. Membrane autopsy is a technique used to identify the cause of low membrane performance (DOW Filmtec 2006). This requires a membrane element to be removed from the plant for destructive analysis. To identify the scales, the solid scale samples are analysed using scanning electron microscopy (SEM) and XRD analytical techniques. The second stage performances have sharply decreased. The module autopsy was ordered. After dissection of the module and unrolling the membrane, a brownish deposit with some black spots appeared on the membrane surface (Figure 4). The RO membrane surfaces were covered by a thin brown film. The nature of the collected scale on the membrane surface (Figure 5) was identified by XRD and infra-red spectroscopy (IRS). The membrane surface was analysed by SEM.

Macroscopic analysis

The first step in the autopsy process is a macroscopic description of the membrane after disassembly. As can be seen in Figure 4(a), the fouled module is clearly observed. The visual inspection of the membrane surface in the feed-reject side shows that the RO membrane surfaces were covered by a thin brown film. The membrane surface in the permeate side is saved by each type of the visible

Figure 5 | Collected deposit on the membrane surface.

contamination at the macroscopic scale. In case of the spacer that separates both RO membranes, the trained fragments are imprisoned into the pores of this one (Figure 4(b)). The scale of these coats may be attributed to the malfunction of pretreatment during the utilization of the unit), and thus, the fouling phenomenon accelerates. These layers characterize the fouled deposit which covers almost the totality of the membrane surface and then engender the increase of the membrane resistance. This is in concordance with the fall of the RO unit performance. To clarify the nature of the fouled species forming this deposit, we will proceed to the characterization of the shape and the chemical nature of the formed deposit using analytical methods such as XRD and SEM.

Deposit identification by XRD and IRS

The XR diffractogram (Figure 6) shows that the membrane deposit is constituted by calcite ($CaCO_3$), coesite and kaolin. The coesite, which is a silica form, can instigate for very fine sand particles. Kaolin is a clay $Al_2Si_2O_5(OH)_4$ with a size less than 0.1 μm. These fine particles may originate from the feed water due to the fact that the well water is surrounded by cost sand, which may cause the transportation of these particles during the intake operation. Consequently, it might be said that the applied pretreatment was not able to trap all fine particles of silica and kaolin. As a solution, the sand and cartridge filters have to be regenerated or replaced more frequently according to the feed water quality. Predominance of calcite in the deposit is further indication of the scaling behaviour (with respect to $CaCO_3$) of the reject flux in the second stage. The IR spectrum (Figure 7) has shown the presence of silica, aluminasilicate (kaolin) (Dupuis *et al.* 2006) carbohydrates (1,040 cm^{-1}) or/and polysaccharide (1,070 and 1,040 cm^{-1}) characteristic bands (Dupuis *et al.* 2006). The presence of organic matter is a clear indication that fouling has an organic origin as well as a mineral one. Similar results were found in a previous report (Moreno *et al.* 2013). This result confirms the presence of organic matter in the deposit

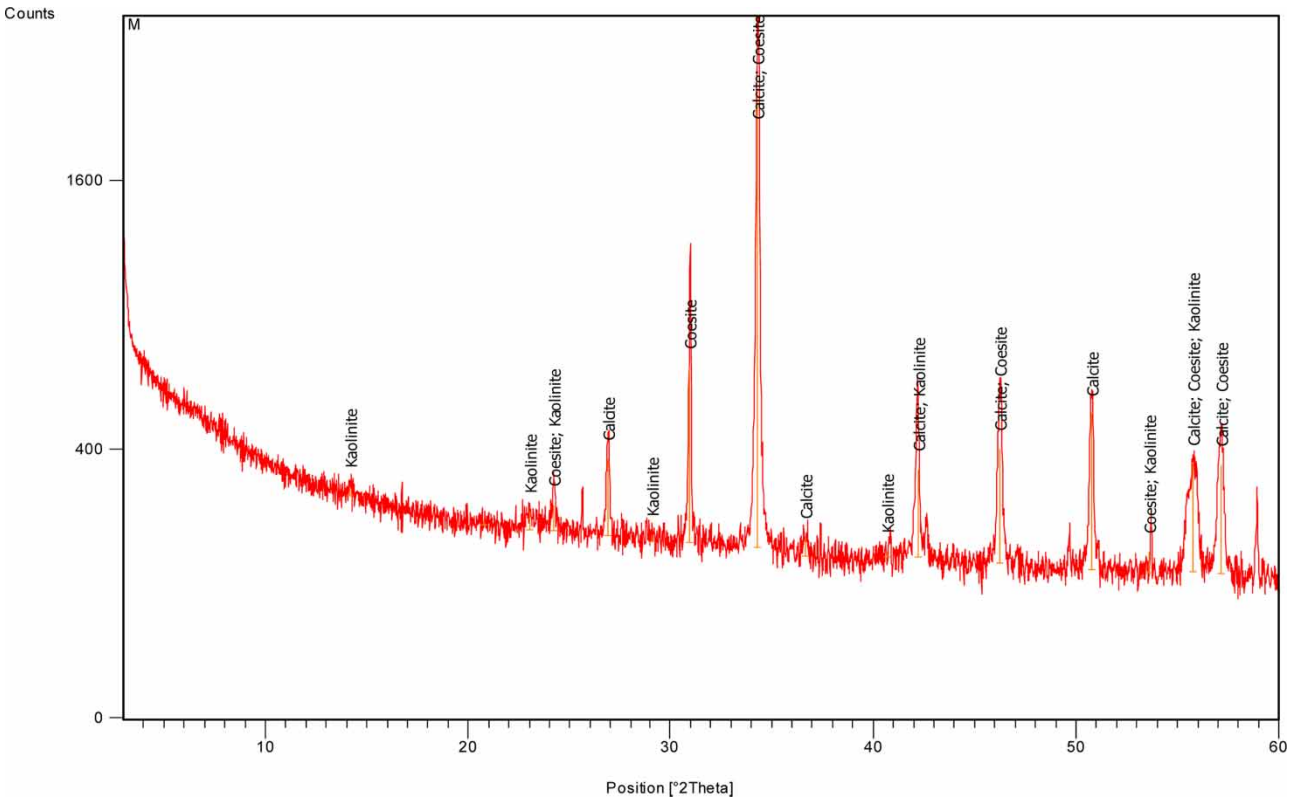

Figure 6 | Deposit X-ray diffractogram.

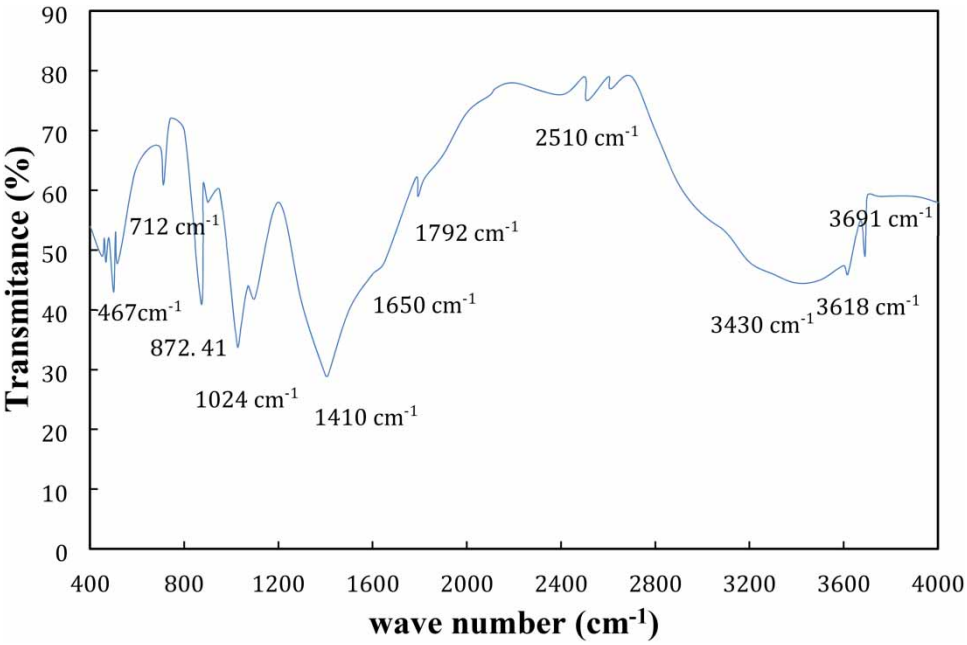

Figure 7 | Deposit IR spectrum.

collected in the membrane surface. It should be pointed out that the peaks relative to the presence of calcite resulting from the precipitation of calcium carbonate in the membrane surface were not found. This can be attributed to the absence of calcite or to its presence with a negligible rate in the total deposit composition.

Membrane surface microscopic examination

The scanning electron microscope is a technique that provides the information on the morphology and the chemical composition of a solid accumulated in the surface of the membrane. Fouled membrane surface has been examined using SEM. Several pictures have been taken, and some of them are shown in Figure 8. In micrograph 3, the formation of a fine coat that surrounds the active coat surface as result of the fouling is observed. This coat is assimilated to a new resistance added to the intrinsic membrane resistivity. Consequently, the performance of the membrane falls drastically. The micrographs reveal that the surface is covered by a rough thick deposit. Moreover, the presence of some mineral crystals on the surface has been detected. These minerals can be attributed to salt precipitation and/or salt leakage upcoming from an ineffective pretreatment. The presence of these crystals is able to damage the membrane and enhance the attraction of the species to the membrane surface (Kang *et al.* 2011). In addition, the need of an extra hydraulic pressure to neutralize the effect of this added resistant layer increases of the energy consumption of the unit (Vincent *et al.* 2014). Therefore, Backwashing and chemical cleaning are inevitable in this case to improve the performance of the RO membranes. Moreover, the presence of the crystals may enhance the germination of the calcium carbonate, and therefore its precipitation due to high calcium concentration in the treated water (Zarga *et al.* 2013).

Energy-dispersive X-ray spectroscopy analysis

Energy-dispersive X-ray spectroscopy analysis of the fouled membrane reveals major elements existence on the membrane surface. The obtained spectrum is shown in Figure 9. The most important peaks on the spectrum are those of iron and manganese oxides. The presence of iron is easily explained by the nature of metal used for the tubing. Manganese most probably is brought by the feed water which has a Mn content of 0.1 ppm that increases to 0.5 ppm in the reject flux of the second stage. Manganese

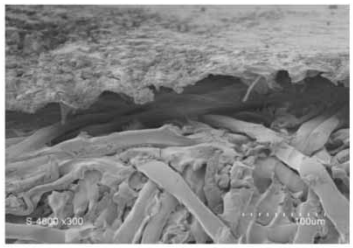

Micrograph 1: Asymmetric membrane structure

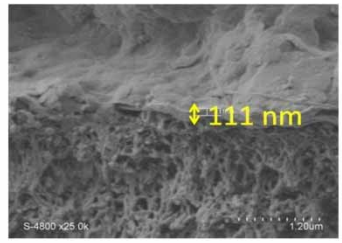

Micrograph 2: Deposit thickness is approximately 111 nm.

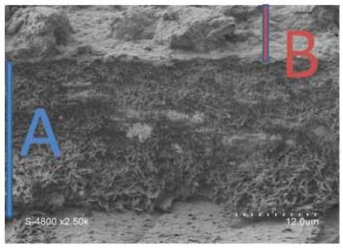

Micrograph 3: Spongy shape membrane (A); deposit layer (B).

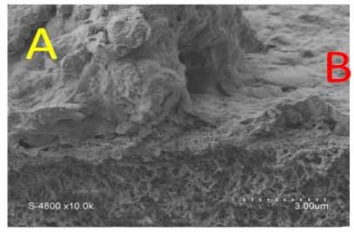

Micrograph 4: Evidence of the deposit roughness. The thickness is not uniform: thickness in region A is much greater than in region B.

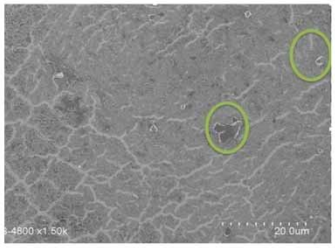

Micrograph 5: Presence of particles of few μm in size.

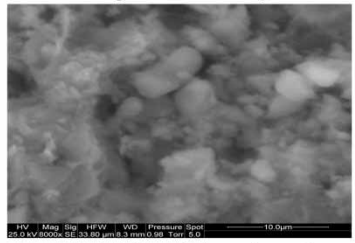

Micrograph 6: Mineral deposit agglomerate.

Figure 8 | SEM photographs of membrane surface.

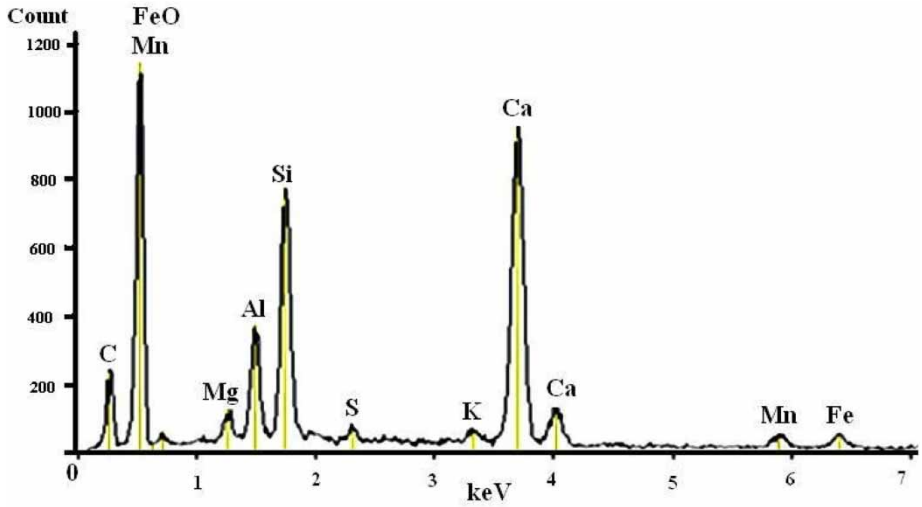

Figure 9 | Fouled membrane energy-dispersive X-ray spectrum.

may react with dissolved oxygen and form highly fouling colloidal matter. Si peak can be due to the presence of SiO_2 infiltrated with the well water towards the membrane. However, the morphological analysis using SEM allows the identification of the silicate crystals. Aluminum and silica peaks are another evidence of alumina-silicate and quartz presence as already revealed by XDR and IRS. The polysulfone nature of the membranes support layer explains the detection of sulfur. The C and O peaks may be due to the organic matter or biologic substances in the deposit. Also, the important peak of aluminum revealed the existence of clay in the deposit. The presence of silicate and clay can be interpreted by a not function of the pretreatment filters. In fact, the pretreatment part has any control system that allows the fouling detection in the level of the cartouches filters and the adequate moment of its replacement. Another reason is that the feed water does not contain a high rate of aluminum. Finally, it is clearly noted the presence of an important pick of Ca is due to the precipitation of calcium carbonate and calcium sulfate.

DIAGNOSIS SUMMARY

Assessment of the scaling/equilibrium/aggressive behaviour has revealed that the second stage reject water is highly scaling with $CaCO_3$ that has a tendency to precipitate instantaneously in the absence of pH adjustment. On the contrary, the produced water is very aggressive. The second stage module autopsy has revealed that the fouling has mineral as well as organic origin. The mineral deposit is composed essentially of coesite, calcite and kaolinite clay. Calcite presence in the deposit clearly indicates that applied chemical inhibition without a pH adjustment was not sufficient to prevent $CaCO_3$ scaling.

To foil scaling, one would suggest acidifying the first stage in addition to the applied chemical inhibition. Furthermore, an efficient membrane acid wash is needed to get rid of any $CaCO_3$ scaling support. Citric acid has given satisfactory results and can replace costly and difficult to handle strong acids such as chlorhydric acid.

Finally, an economical investigation is needed to state whether or not it is pertinent to revamp the damaged unit, use a single stage, or maintain the present running regime in the second stage with a decreases a lower yield (only 18% of the total produced flux) despite a higher pressure demand.

CONCLUSION

The diagnosis of the small RO unit has been undertaken. The unit is a two-stage ROWD unit with a capacity of 45 m^3/h. The second stage of the unit has experienced a sharp decrease in its performance. Presently, this stage modules are contributing to only 18% of unit yield with higher energy consumption.

To assess the scaling tendency, all water fluxes within the desalination unit have been chemically analysed. The MLSI was used for the assessment. The investigation has shown that the second stage reject is highly scaling with respect to calcium carbonate. Most probably, the dosage of antiscalant alone is not sufficient to suppress $CaCO_3$ precipitation. The permeate water was very aggressive. The second stage module autopsy has revealed an intensive mineral as well as organic fouling. The inorganic deposit is basically formed of coesite, calcite and kaolinite. The presence of silica and clay has been explained by a poor filtration operation ahead to the RO modules which was not able to trap very fine feed water suspended matter. The presence of calcite is an indication that the dosage of antiscalant alone without a pH adjustment is not sufficient to suppress $CaCO_3$ precipitation in the second stage membranes. The actual operating conditions which the unit has experienced may not be known. However, a malfunctioning of antiscalant injection even for a very short period would result in irremediable membrane scaling with calcium carbonate. Therefore, a periodic acid wash of the modules becomes necessary.

REFERENCES

Ben Hamouda, S., Hasan Akhtar, F. & Elfil, H. 2014 Diagnosis of small capacity reverse osmosis unit for desalinated tap water. *Desalination and Water Treatment* **52**, 6976–6984.

Boubakri, A. & Bouguecha, S. 2008 Diagnostic and membrane autopsy of Djerba Island desalination station. *Desalination* **220**, 403–411.

DOW Filmtec 2006 *Pilot Study, Seawater Membrane Autopsy*.

Dupuis, T., Ducloux, J., Butel, P. & Nahon, D. 2006 Etude par spectrographie infrarouge d'un ebcroutement calcaire sous galet. *Clay Minerals* **19**, 605–614.

Elfil, H. & Hannachi, A. 2006 Reconsidering water scaling tendency assessment. *AIChE Journal* **52**, 3583–3591.

Elfil, H. & Roques, H. 2001 Role of hydrate phases of calcium carbonate on the scaling phenomenon. *Desalination* **137**, 177–186.

Elfil, H. & Roques, H. 2004 Prediction of the metastable zone in '$CaCO_3$-CO_2-H_2O' system. *AIChE Journal* **50**, 1908–1916.

Elfil, H., Martin-Dominguez, A. & Roques, H. 1998 Contribution to study of scaling phenomena. P.9: study of germination conditions at 30 °C. *Tribune de l'Eau* **594**, 37–62.

Gal, J. Y., Fovet, Y. H. & Gache, N. 2002 Mechanisms of scale formation and carbon dioxide partial pressure influence, Part I: elaboration of an experimental method and a scaling model. *Water Research* **36**, 755–763.

Hannachi, A. 2007 A New Index MLSI for Scaling Assessment. In: *IDA Word Congress on Desalination and Water Reuse*, Grand Canaria, Spain.

Ivnitskya, H., Katza, I., Minzc, D., Shimonid, E., Chene, Y., Tarchitzkye, J., Semiat, R. & Dosoretza, C. 2005 Characterization of membrane biofouling in nanofiltration processes of wastewater treatment. *Desalination* **185**, 255–268.

Kang, N. W., Lee, S., Kim, D., Hong, S. & Hyang Kweon, J. 2011 Analyses of calcium carbonate scale deposition on four RO membranes under a seawater desalination condition. *Water Science and Technology* **64** (8), 1573–1580.

Langelier, W. F. 1936 The analytic control of anti-corrosion water treatment. *Journal – American Water Works Association* **28**, 1500–1521.

Moreno, J., Monclús, H., Stefani, M., Cortada, E., Aumatell, J., Adroer, N., De Lamo-Castellví, S. & Comas, J. 2013 Characterisation of RO fouling in an integrated MBR/RO system for wastewater reuse. *Water Science and Technology* **67** (4), 780–788.

Ning, R., Thomas, L. & Roger, S. 2005 Chemical control of colloidal fouling of reverse osmosis systems. *Desalination* **172**, 1–6.

Stiff, H. A. & Davis, L. E. 1952 A method for predicting the tendency of oil field water to deposit calcium carbonate. *Petroleum Transactions, AIME* **195**, 213–216.

Tran, T., Bolto, B., Gray, S., Hoang, M. & Ostarcevic, E. 2007 An autopsy study of a fouled reverse osmosis membrane element used in a brackish water treatment plant. *Water Research* **41**, 3915–3923.

Vincent, L., Michel, L., Catherine, C. & Pauline, R. 2014 The energy cost of water independence: the case of Singapore. *Water Science and Technology* **70** (5), 787–794.

Zarga, Y., Ben Boubaker, H., Ghaffour, N. & Elfil, H. 2013 Study of calcium carbonate and sulfate co-precipitation. *Chemical Engineering Science* **96**, 33–41.

First received 8 December 2016; accepted in revised form 31 March 2017. Available online 28 April 2017